

Diffused Quantum Well Solar Cells

Y. Cheng, Alex S.W. Lee and E. Herbert. Li

Department of Electrical and Electronic Engineering
The University of Hong Kong, Pokfulam Road, Hong Kong

Abstract - An alternative multi-bandgap solar cell made of diffused quantum well (DFQW) as the absorber is proposed here. The modeling of the spectral response and energy conversion efficiency of the solar cell will be shown. Significant enhancement in energy conversion efficiency is demonstrated when compared to that of the single bandgap cells.

I. INTRODUCTION

Incorporating quantum wells into the absorption layer of the solar cell as an alternative to conventional multi-bandgap approach has been proposed¹. Significant enhancements in short circuit current and energy conversion efficiency have already been demonstrated by using variable well width AlGaAs/GaAs p-i-n multi-quantum well (MQW) photodiodes². The results show prospect for using QW as the active absorber in the solar cell. We propose here an alternative way of improving the efficiency by using diffused quantum well (DFQW) system with equal well width, which is presumably easier to fabricate than the QW structure with variable well width. The different bandgaps of the QW system can be selectively modified by employing suitable masks to control the extent of ion implanted into the required region. The efficiency of the DFQW cell compared to that of the single-band-gap is shown to be increased. The calculations on spectral response and energy conversion efficiency are based on ideal solar cell models.

II. MODEL

The proposed structure, depicted in Fig.1, consists of $\text{Al}_x\text{Ga}_{1-x}\text{As}/\text{GaAs}$ and $\text{GaAs}/\text{In}_y\text{Ga}_{1-y}\text{As}$ DFQW system in the depletion region of a heterostructure solar cell. We choose $\text{Al}_x\text{Ga}_{1-x}\text{As}/\text{GaAs}$ QW system because of its best understood well properties among the III-V materials. The choice of $\text{GaAs}/\text{In}_y\text{Ga}_{1-y}\text{As}$ is for a lower absorption bandgap range which results in an increase in the overall absorption wavelength and an extended spectral response.

In order to have a larger area of photon collection, the front contact of the solar cell is groove-etched. The DFQW system consists of 10 periods of barrier/well with the well width=100Å and barrier

width=200Å. A possible way to fabricate the proposed MQW system with different bandgaps is to use a mask during ion implantation as shown in Fig.2. After implantation, the mask shown in the figure will be removed.

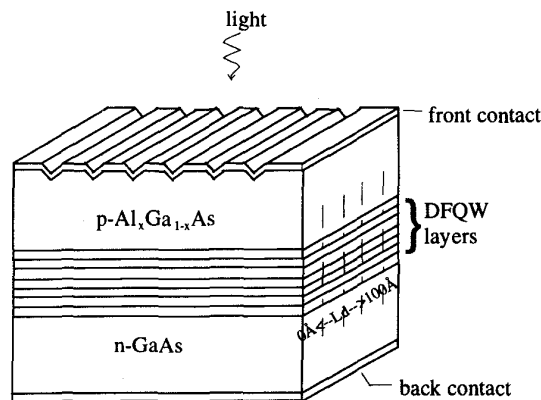


Fig.1. Schematic representation of a diffused quantum well solar cell. Bandgap energy of the DFQW layers varies as the diffusion length of the implanted ions.

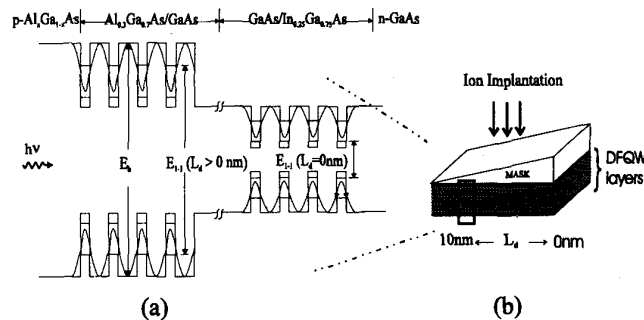


Fig.2. Schematic representation of the DFQW layers with well width=10nm and barrier=20nm. (a) Bandgap structure is shown in 90 degrees rotation. Curve lines represent the bandgaps after diffusion. (b) The bandgaps are modified by using ion implantation process.

The choice of aluminum mode fraction around 0.3 is from a common practice. The indium mode fraction=0.25 is to avoid reaching the critical layer thickness³. We let the barrier width doubles that of the well is to minimize the interference from adjacent wells so that we can use the single QW model to calculate the absorption coefficient.

In our system, the well width of 100Å is based on the maximum diffusion length of the implanted ions, $L_{d,ion}=100\text{\AA}$ and is determined from the following MQW diffusion model⁴ for the composition profile:

$$w(z) = \frac{w_0}{2} \left\{ \sum_{i=1}^n \left[\operatorname{erf} \left(\frac{z-a_i}{2L_d} \right) - \operatorname{erf} \left(\frac{z-b_i}{2L_d} \right) \right] + \left[2 - \operatorname{erf} \left(\frac{z-c_1}{2L_d} \right) - \operatorname{erf} \left(\frac{z-c_2}{2L_d} \right) \right] \right\}, \quad (1)$$

where w_0 is the as-grown Al (or In for InGaAs) concentration in both the barrier and the cladding layer; n is the number of as-grown barriers within the MQW core; $\operatorname{erf}(z)$ represents the error function; a_i and b_i represent the i^{th} as-grown barrier within the MQW core and are the left and right interface positions respectively; c_1 and c_2 are the position of the interfaces between the cladder and the core. In Fig. 3, we can see how the bandgaps vary with different diffusion length.

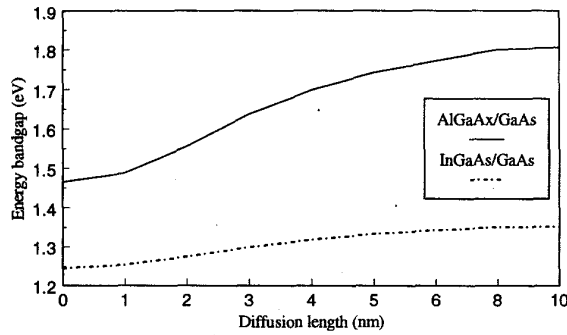


Fig. 3. Energy bandgap varies as a function of diffusion length.

The spectral response was first calculated by solving the minority carriers continuity equations in a fieldless model⁵ at room temperature to obtain the photocurrent J_n and J_p from the p and n region.

$$D_p \frac{d^2 \Delta n_p}{dx^2} + \alpha F \exp(-\alpha x) - \frac{\Delta n_p}{\tau_n} = 0, \quad (2)$$

$$D_n \frac{d^2 \Delta p_n}{dx^2} + \alpha F \exp(-\alpha x) - \frac{\Delta p_n}{\tau_p} = 0, \quad (3)$$

The boundary conditions for p-type material, $\text{Al}_x\text{Ga}_{1-x}\text{As}$ are:

$$D_p \frac{d\Delta n_p}{dx} = S_p \Delta n_p, \quad (x=0) \quad (4)$$

$$\Delta n_p = 0, \quad (x=x_f-x_p) \quad (5)$$

The boundary conditions for n-type material, GaAs are:

$$D_n \frac{d\Delta p_n}{dx} = S_n \Delta p_n, \quad (x=H) \quad (6)$$

$$\Delta p_n = 0, \quad (x=x_f+w+x_n) \quad (7)$$

where $D_{p,n}$ are diffusion constants of p- and n-type materials. p_n, n_p are minority carriers concentration. λ and F are the wavelength and photon flux of incident light respectively. x_f is the depth of p-layer and w is the width of the MQW layer. x_n and x_p are the extensions of depletion layer into the n- and p-sides respectively. H is the depth of the structure from front to the back contact. $\tau_{p,n}$ are the lifetimes of the minority carriers. $S_{p,n}$ are the surface recombination velocities. The parameters used for calculations are shown in the following Table:

TABLE I
INPUT PARAMETERS FOR MODELING

Material	S(cm.s ⁻¹)	L(μm)	τ(ns)	N(cm ⁻³)	Ref.
p-Al _{0.37} Ga _{0.63} As	10 ⁶	2.3	3.47	1x10 ¹⁷	6
n-GaAs	∞	2.2	7.9	1x10 ¹⁷	7

By solving the above equations with their respective boundary conditions, we obtain the photocurrent J_n and J_p . To these, we add the photocurrent contributed from within the depletion region by modifying J_{dep} as follows,

$$J_{dep} = qF \exp(-x_j \alpha_j) \left[1 - \exp(-\alpha_p x_p) - M(\alpha_1 L_1 + \alpha_2 L_2) - \alpha_n x_n \right], \quad (8)$$

where the first exponential factor is the attenuation of the light through the undepleted p layer; α_p and α_n are the absorption coefficients at λ of the p and n region; α_1 and α_2 are the absorption coefficients of the two QW systems; L_1 and L_2 are the widths of the QW systems and M the number of QWs.

The assumptions made are that both sides of the junction are taken to be uniform in doping and the reflectance is assumed to be zero for ideal case. The total short-circuit current density then becomes,

$$J_{sc}(\lambda) = J_n(\lambda) + J_p(\lambda) + J_{dep}(\lambda), \quad (9)$$

Finally, the spectral response is calculated from the following equation,

$$SR(\lambda) = \frac{J_{sc}(\lambda)}{qF(\lambda)}, \quad (10)$$

The absorption coefficient we used for bulk $Al_xGa_{1-x}As$ and GaAs are published data from ref. 9 and that for QW system, we calculated from the band mixing QW model¹⁰.

The energy conversion efficiency, η , of the solar cell is given by: $\eta = J_m V_m / P_{in}$, where J_m and V_m are the optimum current density and voltage, respectively, which are both given at maximum power. P_{in} is the incident power per unit area. These are calculated on the basis of a simple superposition model which is also used in Ref. 1. The current density, J_m , is given by:

$$J_m = \frac{qn_{ph}(E_g)}{1 + (kT/qV_m)}, \quad (11)$$

where q is the electric charge; $n_{ph}(E_g)$ is the number of photons with energy greater than the effective bandgap for absorption per unit area per second. k is the Boltzmann constant; T is the temperature, where we used 300K in the calculation.

V_m is solved from the following equation: $V_m = V_{oc} - kT \ln[1 + (qV_m/kT)]/q$, where V_{oc} , the open circuit voltage is given by $V_{oc} = [E_b - kT \ln(A/J_{sc})]/q$. In which, E_b is the barrier bandgap, which we assume to be the bulk bandgaps, and A is the parametrization in the dark current density¹¹.

III. RESULTS

With the addition of the DFQW system, the absorption range of energy is increased, provided that the incident energy is higher than E_{1-1} , as depicted on Fig.2. Since the resulting bandgap energies vary as the diffusion lengths, we can tailor the bandgaps of the MQW from 1.25 to 1.8eV by adjusting the diffusion lengths with the use of a mask in the proposed structure. The resulting spectral response of the solar cell with and without the DFQW system are shown in Fig.4. Significant enhancement in spectral response is shown with the adding of the DFQW system.

In Fig.5, we can see the improvement of the energy conversion efficiency over the conventional single bandgap cell. The efficiency is increased by about 5% in average. In the extreme case, where the bandgap around 1.44eV which is also the theoretical optimal bandgap for solar cell, the efficiency is even almost 10% higher.

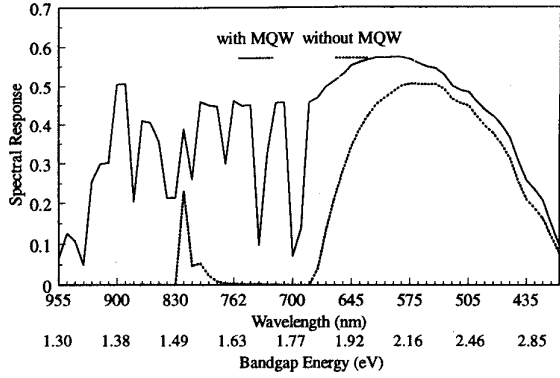


Fig. 4. Spectral response of the DFQW solar cell.

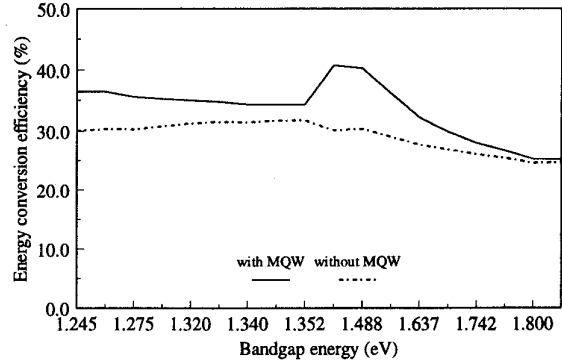


Fig. 5. Comparison of the energy conversion efficiency of the DFQW solar cell and the conventional single bandgap cell.

IV. CONCLUSION

To conclude, with the spectral response and energy efficiency enhancement demonstrated by our proposed solar cell structure, and in view of the advances in the MBE and MOCVD growth techniques, DFQW solar cell could provide a new approach to the high efficiency solar cell.

ACKNOWLEDGMENT

One of the authors (Y.C.) would like to acknowledge C.Y. Chan and C.H. Choy for their helpful discussions and suggestions. This work is supported by the HKU-CRCG grant.

REFERENCES

- [1] K.W.J. Barnham and G. Duggan, "A new approach to high-efficiency multi-band-gap solar cells", *J. Appl. Phys.* **67**, 3490 (1990).

- [2] K.W.J. Barnham, B. Braun, J. Nelson, M. Paxman, C. Button, J.S. Roberts, and C.T. Foxon, "Short-circuit current and energy efficiency enhancement in a low-dimensional structure photovoltaic device", *Appl. Phys. Lett.* **59**, 135 (1991)
- [3] J.Y. Yao, T.G. Andersson and G.L. Dunlop, "Microstructures and critical thicknesses of $\text{In}_x\text{Ga}_{1-x}\text{As}/\text{GaAs}$ strained-layer structures", *Semicond. Sci. Technol.* **9**, 1086 (1994)
- [4] E.H. Li, B.L. Weiss and K.S. Chan, "Eigenstate and absorption spectra of interdiffused $\text{AlGaAs}/\text{GaAs}$ multiple QW structures", *J. Appl. Phys.* (submitted to *Phys. Rev. B*)
- [5] H.J. Hovel, *Semiconductors and Semimetals* (Academic, New York, 1975), Vol. 11.
- [6] Adachi, *Properties of Aluminum Gallium Arsenide* (INSPEC, London, 1993).
- [7] H.C. Casey, Jr., B.I. Miller and E. J. Pinkas, *Appl. Phys.*, **44**, 1281 (1972).
- [8] M. Paxman, J. Nelson, B. Braun, J. Connolly, and K.W.J. Barnham, C.T. Foxon and J.S. Roberts, "Modeling the spectral response of the quantum well solar cell", *J. Appl. Phys.*, **74**, 614 (1993).
- [9] D.E. Aspnes, S.M. Kelso, R.A. Logan, and R. Bhat, "Optical properties of $\text{Al}_x\text{Ga}_{1-x}\text{As}$ ", *J. Appl. Phys.*, **60**, 754 (1986).
- [10] E.H. Li, B.L. Weiss, and K.S. Chan, "Effect of interdiffusion on the subbands in an $\text{Al}_x\text{Ga}_{1-x}\text{As}/\text{GaAs}$ single-quantum-well structure", *Phys. Rev. B*, **46**, 15181 (1992).
- [11] C. H. Henry, "Limiting efficiencies of ideal single and multiple energy gap terrestrial solar cells", *J. Appl. Phys.*, **51**, 4494 (1980).